Desalination and Water Treatment
www.deswater.com

doi: 10.5004/dwt.2017.1490

60 (2017) 180–187
January

Kinetic and equilibrium isotherm studies of ammoniacal nitrogen adsorption onto sugarcane bagasse from wastewater

Khushboo Bhavsar[a,*], Nisha K. Shah[b], Divya Buha[b], Krishna Atalia[b]

[a]*Department of Environmental Science, School of Science, Gujarat University, Ahmedabad-380001, India, Mobile: 07359567267; email: k.bhavsar8384@gmail.com*
[b]*Department of Chemistry, School of Science, Gujarat University, Ahmedabad-380001, India*

Received 7 October 2015; Accepted 9 July 2016

ABSTRACT

In this research, Sugarcane Bagasse (SB), an agricultural waste, available in large quantities was used as low-cost adsorbent for removal of ammoniacal nitrogen form the wastewater. Batch operation was used to study the equilibrium behavior of the SB. Kinetic and isotherm studies were carried out by considering the effects of various parameters, such as pH, contact time, adsorbent dosage, temperature, particle size and agitation rate. The maximum adsorption was attained at the various optimum parameters. The obtained materials were characterized by scanning electron microscopy analysis and Fourier Transform infrared spectroscopy (FT-IR). The equilibrium data for the adsorption of ammoniacal nitrogen on SB was tested with various adsorption isotherm models such as Langmuir, Freundlich and Temkin. The Langmuir isotherm model is found to be the most suitable one for the adsorption and the maximum adsorption capacity obtained is 97%. Adsorption kinetics data were tested using pseudo-first-order and pseudo-second-order. Kinetic studies showed that the adsorption followed a pseudo-second-order reaction. The results indicate that SB can be an attractive option for ammoniacal nitrogen removal from industrial wastewaters.

Keywords: Ammoniacal nitrogen; Adsorption; Isotherm; Kinetic studies; Sugarcane bagasse

1. Introduction

Ammoniacal nitrogen (NH_4–N), nitrite (NO_2) and nitrate (NO_3), are the nutrient compounds often present in diversified nature of waters and wastewater and these end up in natural water bodies and drinking water. Usually, the ammonia pollution occurs due to the animal feeds, food additives, cleaning agents and effluents from industries manufacturing fibers, plastics, explosives, paper and rubber [1]. Although, Nitrogen is an essential nutrient to all living organisms [2] but can also be harmful to organisms. No doubt, protein is a fundamental building block of plant and animal proteins but anything in excess is always a toxic material to the environment or organism. Typically, proteins in living organisms contain about 16% nitrogen. Animal and human wastes too have substantial amounts of nitrogen incorporated into organic molecules such as urine; mostly in the form of urea [3]. Extensive microbial action on urea molecule releases ammonia which in turn can promote the growth of algae. Algal growth decline the dissolved oxygen required for aquatic life if the concentration of NH_4–N exceeds 0.3–0.5 mg L^{-1} [4]. The removal of wastewater NH_4–N is important in the alleviation of environmental problems including eutrophication, corrosion and fouling [5]. The removal of NH_4–N can be accomplished by biological, physical, chemical, or a combination of these methods. Available technologies include adsorption, chemical precipitation, membrane filtration, reverse osmosis, ion exchange, air stripping, breakpoint chlorination and biological nitrification and denitrification [6]. Conventional wastewater treatment technologies, however, are expensive to build and also have associated operational and maintenance

---

[*] Corresponding author.

problems. From a practical perspective, adsorption is one of the most promising techniques. Adsorbents such as activated carbon, zeolite, agricultural waste, etc are effective and frequently used for the removal of ammoniacal nitrogen. Recently, higher tendencies of using adsorbent prepared from waste generated in large quantities, easily available and cheap to solve the problem of treatment of wastewater. Removal of ammoniacal nitrogen form aqueous solution has been carried out using activated carbon, marine flora like *Posidonia oceanica,* green algae, saw dust, microalgae, zeolite and many more adsorbents. Additional emphasis is made to agricultural waste material for preparation of adsorbent as they are ecofriendly and due to their unique chemical composition which makes them as a promising material for the removal of ammonium from the system [7].

For above mentioned reasons the efforts were attempted to investigate the adsorption capacity of ammonium ions by sugarcane bagasse (SB) by optimizing the parameters like pH, contact time, adsorbent dosage, temperature, particle size and agitation rate. Additionally, kinetics and equilibrium isotherm models were used to fit experimental data.

2. Materials and methods

2.1. Reagents and chemicals

All the chemicals used in the study were of analytical grade. Distilled water was obtained from a glass distillery. The same distilled water was used to prepare all the solutions. Working solutions from respective standard solutions were also freshly prepared using double distilled water.

2.2. Wastewater

The wastewater used in this study was obtained from a local dye and dye intermediates industry. Ammonium ions are subjected to escape due to its unstable nature. Waste water was preserved in the air-tight sealed bottles and preserved by adding H_2SO_4 (@ 0.8 ml per liter of wastewater) and at 4°C for maximum of 7 d. Thorough analysis of the wastewater was carried out using standard methods [8] to know the characteristic of it.

2.3. Biomass preparation

SB was collected from the local juice centre and boiled for 30 min to remove the soluble sugars. Washed-off bagasse was dried in a hot air oven at 70°C for 24 h and ground into fine particles. It was sieved to pass uniform size of less than 50–60 µm [9]. The prepared adsorbent was stored in a airtight bags for further experimental use.

2.4. Characterization of adsorbent

To find the data on the main chemical groups present on the surface of the SB particles and to detect probable alterations of the active sites in SB during ammonium adsorption, Fourier transform infrared spectroscopy (FTIR) (Model: Shimadzu 8,400 s) was used [10]. For the analysis, KBr pellets were prepared containing SB. The spectrum was recorded from 4,000 to 400 cm^{-1}.

The surface morphology of the material was examined using scanning electron microscopy (SEM) (Model: ESEM EDAX XL-30, Philips, Netherlands) under 5 kV electron acceleration voltage.

2.5. Equilibrium experiments

The adsorption experiments were conducted for the determination of pH, contact time, adsorbent dosage, temperature, particle size and agitation rate. Also, these equilibrium parameters were adopted to study the kinetics and for the selection of an isotherm. The influence of pH (2–12), contact time (30–360 min), Adsorbent dosage (0.2–2 gm), temperature (25°C to 55°C), particle size (10–50 mm) and agitation rate (50–500 rpm) were evaluated during the present study in a 250 ml screw-cap conical flask [11]. The initial pH of the dye solutions were adjusted to the desired values by adding few drops of 0.1 M HCl or 0.1 M NaOH aqueous solutions. All the flasks for the experiments were agitated on temperature controlled mechanical shaker.

After the stipulated optimum contact time the flasks were removed from the mechanical shaker and content was filtered through whatman filter paper no 42. The filtrate was analyzed for NH_4–N by Kjeldhal method. Each experiment was conducted three times and average values are reported.

The % removal of NH_4–N was calculated using the following equation [12]:

$$\text{Removal}\ (\%) = \frac{(C_i - C_e)}{C_i} * 100 \tag{1}$$

where C_i = Initial concentration of NH_4–N (mg l^{-1}), C_e = Equilibrium concentration of NH_4–N (mg l^{-1}).

2.6. Isotherm models

The experimental adsorption data were analyzed using the Langmuir and Freundlich models to determine the best model that characterize the adsorption mechanism.

2.6.1. Langmuir isotherm

Linear form of Langmuir model is expressed by Eq. (2):

$$\frac{C_e}{q_e} = \frac{C_e}{Q} + \frac{1}{Qb} \tag{2}$$

where C_e is equilibrium concentration of C_r (mg L^{-1}), q_e is amount of C_r adsorbed at equilibrium (mg g^{-1}), a and b are Langmuir constants related to adsorption capacity and rate of adsorption capacity, respectively. The linear plot of C_e/q_e vs. C_e.

The shape of the Langmuir isotherm was investigated by the dimensionless constant separation term (R_L) to determine high affinity adsorption. R_L was calculated as per Eq. (3).

$$R_L = \frac{1}{1 + bC_0} \tag{3}$$

R_L indicates the type of isotherm to be irreversible ($R_L = 0$), favorable ($0 < R_L < 1$), linear ($R_L = 1$) (or) unfavorable ($R_L > 1$). In the present investigation, the *RL* value (i.e., 0.075) was less than one for C_r concentration range studied, which shows the adsorption process was favorable.

2.6.2. Freundlich isotherm

Linear form of Freundlich model is expressed by Eq. (4):

$$\log q_e = \log K_F + \frac{1}{n}\log C_e \tag{4}$$

where K_F is measure of adsorption capacity (mg g^{-1}) and *n* is adsorption intensity. 1/*n* values indicate the type of isotherm to be irreversible ($1/n = 0$), favorable ($0 < 1/n < 1$), unfavorable ($1/n > 1$).

2.6.3. Temkin isotherm

This isotherm contains a factor that explicitly taking into the account of adsorbent–adsorbate interactions. By ignoring the extremely low and large value of concentrations, the model assumes that heat of adsorption (function of temperature) of all molecules in the layer would decrease linearly rather than logarithmic with coverage [13]. As implied in the equation, its derivation is characterized by a uniform distribution of binding energies (up to some maximum binding energy) was carried out by plotting the quantity sorbed q_e against $\ln C_e$ and the constants were determined from the slope and intercept. The model is given by the following equations [14]:

$$q_e = \frac{RT}{b}\mathrm{In}\left(A_T c_e\right) \tag{5}$$

$$q_e = \frac{RT}{b_T}\mathrm{In}\ A_T + \left(\frac{RT}{b_T}\right)\mathrm{In}\ C_e \tag{6}$$

$$B = \frac{RT}{b_T} \tag{7}$$

$$q_e = B\ \mathrm{In}\ A_T + B\ \mathrm{In}\ C_e \tag{8}$$

where A_T =Temkin isotherm equilibrium binding constant (L g^{-1}), b_T = Temkin isotherm constant, *R*= universal gas constant (8.314 J mol^{-1} K^{-1}), *T*= Temperature at 298 K, *B* = Constant related to heat of sorption (J mol^{-1}).

2.7. Kinetic studies

A linear form of pseudo-first-order model was described by Lagergren [15] in the form:

$$\log\left(q_e - q_t\right) = \frac{\log q_e - k_1 t}{2.303} \tag{9}$$

A linear plot of log ($q_e - q_t$) against time allows one to obtain the rate constant. The Lagergren first order rate constant (k_1) and q_e determined from the model along with the corresponding correlation coefficients.

The pseudo-second-order kinetics may be expressed in a linear form as [15,16]:

$$1/q_t = 1/k_2 q_e^{\,2} + 1/q_e t \tag{10}$$

where the equilibrium adsorption capacity (q_e), and the second order constants k_2 (g mg^{-1} h) can be determined experimentally from the slope and intercept of plot t/q_t vs. *t* .The k_2 and q_e determined from the model along with the corresponding correlation coefficients.

3. Results and discussion

3.1. Characterization of adsorbent

3.1.1. FTIR study and adsorption mechanism

SB is a cellulose matrix, which has various binding sites. These includes, carboxyl (–COOH) and hydroxyl (–OH) groups. FTIR spectra of SB before and after ammoniacal nitrogen adsorption are shown in Fig. 1. The spectra (a) has comparatively medium peaks than those deep ones obtained after (b) ammonium ions adsorbed onto SB.

The peaks between 3,100 and 3,500 cm^{-1} has increased in depth and number of peaks had also increased. This indicates there was additional (–NH) Primary and secondary amine stretching due to the ammoniacal nitrogen adsorption onto the surface. Also, peaks of 2931.60 and 2488.45 cm^{-1} were added to the spectra after the adsorption which indicates the Imines (>C= NH) bending. A distinct 2100.34 cm^{-1} peak shows a nitrile (C=N) stretching. Additionally, peaks between 1,600 and 1,500 cm^{-1} proved an additional amide bending which appeared after adsorption process. Furthermore, peaks between 1,350 and 1,450 cm^{-1} in the spectra (b) proved the existence of nitro group. Also, new peaks added in the range 1,050–1,150 cm^{-1} and 650–900 cm^{-1} showed shift of (C-N) amine stretching and N-H wag from medium to strong appearance, respectively.

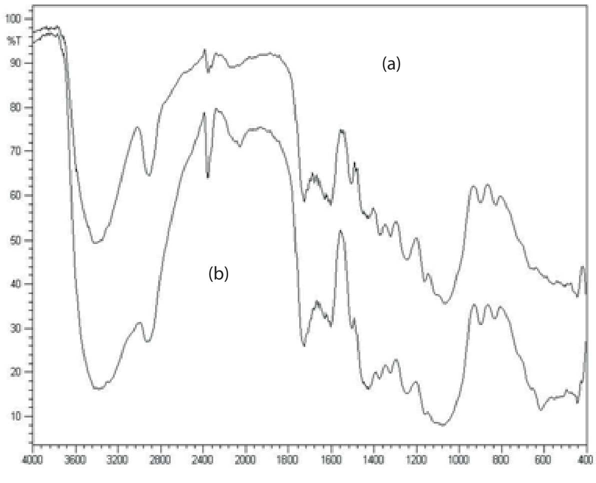

Fig. 1. FT-IR spectrum of SB (a) before and (b) after adsorption of ammoniacal nitrogen onto SB.

Similar additional peaks were observed by many researchers working with the numerous adsorbent for the removal of ammoniacal nitrogen from aqueous solutions.

3.1.2. Scanning electron microscopy

Figs. 2(a) and (b) shows the SEM micrographs of SB before and after the adsorption of ammoniacal nitrogen. Figs. 2(a) and (b) images obtained revealed two main morphological features: fiber structure and pith. Amplification of the pith are shown in the Figs. 2(a) and (b). There is a change observed on the surface of the SB before and after adsorption of ammoniacal nitrogen. Before adsorption, the surface of the magnified pith cell surfaces show sharp edge platy structures grouped together as a clump. The surface has an irregular arrangement of cells which makes many trenches between the platy structures favoring the adsorption process.

Later, we observe in Fig. 2(b) the irregular arrangement comprising fractures and slits were observed to get occupied and plain surfaces with evenly formed areas were perceived on the surface of the biosorbent.

3.2. Equilibrium experiments

3.2.1. Influence of pH

Results of biosorption studies at pH 2–12 are presented in Fig. 3. Previous studies indicate the pHpzc (point of zero charge) of bagasse was found to be about 5.0 [17]. The equilibrium biosorption capacity was minimum at pH 2, with a gradual increase of 20% till pH 5. The abrupt increase (30%) in the adsorption capacity was observed between pH 5 and pH 6 and reached a maximum adsorption of ammonium ion at pH 8. The reason for such a continuing change in the efficiency of the adsorbent is changes in the charges on the surface of the adsorbent. At lower pH, the surface becomes positively charged, thus the amount of ammonium gets adsorbed decreased. Whereas, with increasing pH the positive charges gets replaced by negative charges this reduces the adsorption efficiency of SB.

A similar trend was observed for the biosorption studies of ammonium ions from aqueous solution onto sawdust [18]. At lower pH, the positively charged surface enhances the amount of adsorption of ammonium ions. A change in adsorption capacity is observed with the change in surface charges of the adsorbent.

3.2.2. Influence of contact time

Fig. 4 shows the plot which reveals the effect of contact time on SB. Adsorption of ammonium ions were measured for the range of 30 to 180 min. The adsorption rate was higher at the beginning. Nearly, 86% removal was observed in first 60 min. This is possibly due to large surface areas available for the ions to get adsorbed. Later a gradual stability was

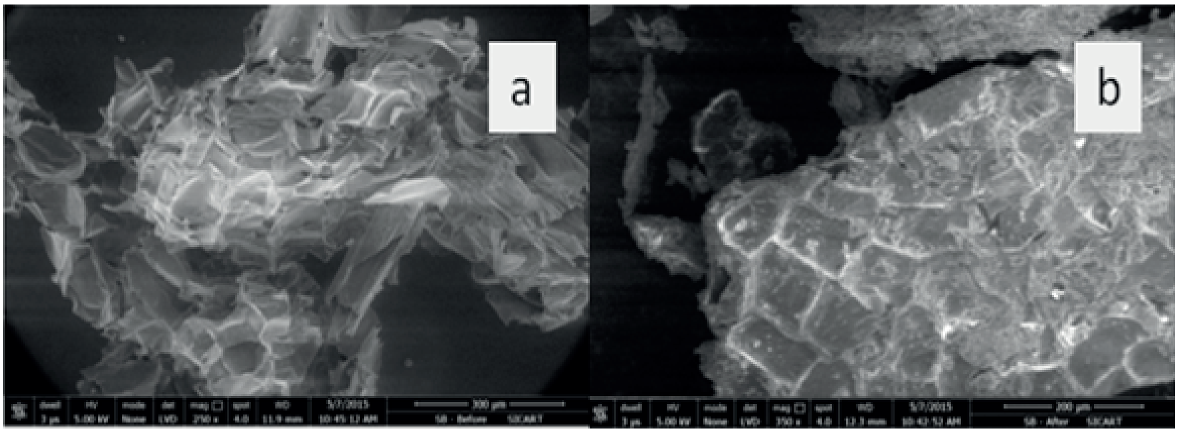

Fig. 2(a) and (b). SEM images showing the surface morphology of SB (a) before and (b) after adsorption of ammoniacal nitrogen onto SB.

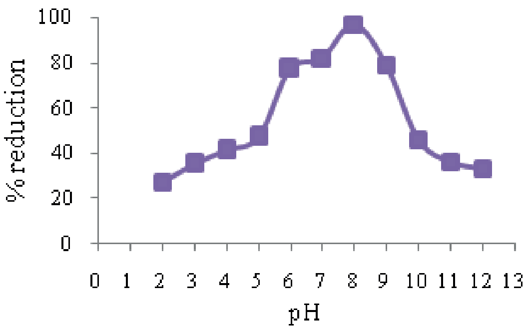

Fig. 3. Influence of pH on the adsorption capacity onto SB.

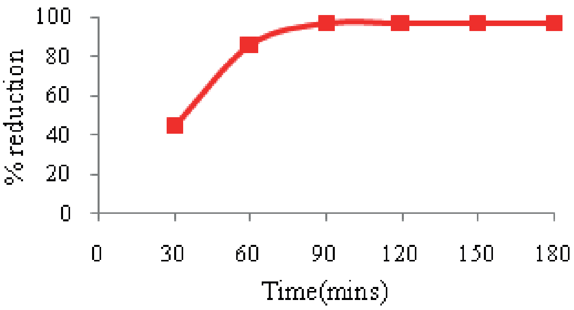

Fig. 4. Influence of contact time on the adsorption capacity onto SB.

attained with the maximum adsorption of 97% after 90 min of contact time. This can be due to the availability of a great number of vacant sites for adsorption in initial stages and remaining vacant sites were complex to be occupied at later stages of adsorption, and also likely due to the repulsive forces between ammonium ion and surface molecules of SB.

Comparable results were obtained in a equilibrium and kinetic study conducted for adsorption of nickel from aqueous solution onto bael tree leaf powder [19].

3.2.3. *Influence of adsorbent dosage*

The influence of adsorbent dosage was studied by varying the sorbent dosage amounts from 0.2 to 2 gm l^{-1}. Fig. 5 shows the adsorption of ammonium ions on SB with different quantities of adsorbent dosage. The increase of 0.2 to 1.2 gm l^{-1} in adsorbent dosage there was a rise of 85.11% in adsorption capacities of SB. In further increase of adsorbent dosage there was no remarkable increase in the adsorption capacity. The substantial increase in the adsorption with the increase of adsorbent dosage is due to the greater availability of the surface area at higher concentration of the adsorbent [20].

Similar increase in adsorption capacities of adsorbent with increase in adsorbent dosage were obtained while working with sawdust as adsorbent for the removal of TDS form the wastewater [21].

3.2.4. *Influence of temperature*

The effect of temperature on adsorption capacity of the adsorbent was studied at 25°C, 35°C, 45°C and 55°C and the results were shown in Fig. 6. Rapid increase of 55% and then after reaching an optimum adsorption capacity of 97% when adsorption process was observed at 45°C temperature, there was a sudden decrease in adsorption capacities of SB. This behavior of the adsorbent suggests that the process is endothermic at lower temperatures and is chemically active. Whereas, with an increase in temperature the process showed a contrasting process of being endothermic with physical adsorption dominating the system. The reason behind the decreasing adsorption with the increasing temperature is the highly energized ammonium molecules and their over-rated mobility resulting escaping of the ions from the binding sites.

Distinct results were observed by several researchers [22] while working with biosorption of acid orange 52 dye by Paulownia *tomentosa* Steud. leaf powder as a low cost natural adsorbent.

3.2.5. *Influence of particle size*

Fig. 7 shows the influence of varying particle sizes from 10 to 50 mm in the process of adsorption of ammoniacal nitrogen using SB. An increase in particle size decreased the percent removal. At a fixed adsorbent dosage, the decrease in particle size increases the ammoniacal nitrogen adsorption capacities. The increase in the adsorption capacities by smaller particles was due to the greater accessibility to pores and to the greater surface area for bulk adsorption per unit mass of the adsorbent [23].

Similar trend was observed on removal of Cr (VI) by using *Pitchellobium dulce* benth [24].

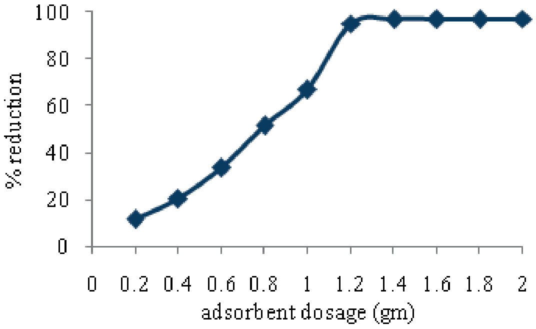

Fig. 5. Influence of adsorbent dosage on the adsorption capacity onto SB.

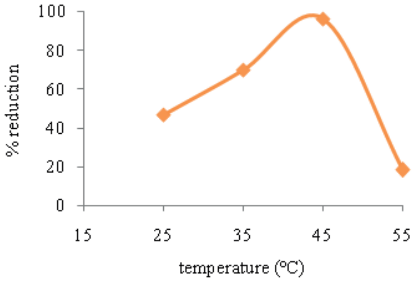

Fig. 6. Influence of temperature on the adsorption capacity onto SB.

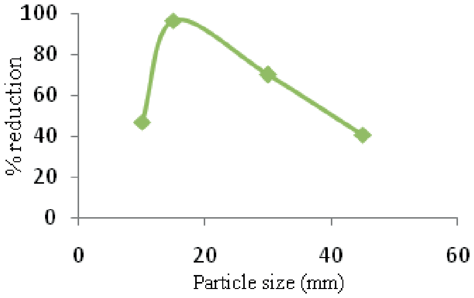

Fig. 7. Influence of particle size on the adsorption capacity onto SB.

3.2.6. *Influence of agitation rate*

The adsorption rate of ammonium ions was checked at different RPM's (50 to 500 rpm) for an initial concentration of 1,500 mg l^{-1} for optimum time duration. The effect of agitation on adsorption rate of ammonium ions is shown in Fig. 8. As can be seen the adsorption rate was highly influenced by the agitation rate. There was a high correlation between agitation and adsorption. With the increase in agitation rate, the contact rate between the adsorbate and adsorbent increases. Agitation increased the mobility of the system and thereby the adsorption rate was also increased.

Similar outcomes were observed working with the commercially available GAC for removal of C_r from aqueous solutions [25].

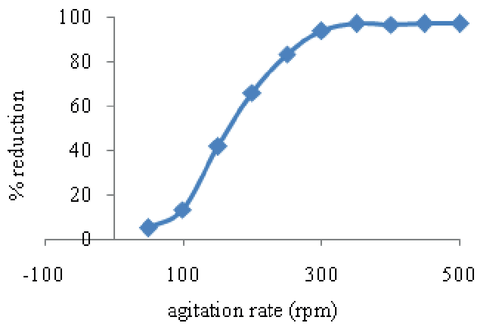

Fig. 8. Influence of agitation rate on the adsorption capacity onto SB.

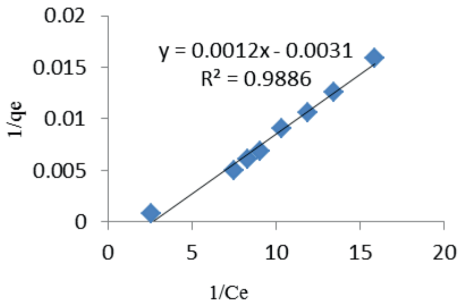

Fig. 9. Langmuir isotherm plot.

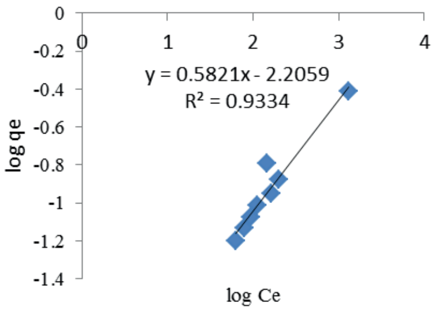

Fig. 10. Freundlich isotherm plot.

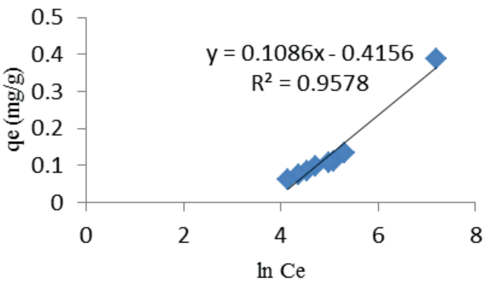

Fig. 11. Temkin isotherm plot.

3.3. Isotherm models

Adsorption isotherms are mathematical models that describe the adsorbate species among liquid and adsorbent, based on a set of assumptions that are mainly related to the heterogeneity/homogeneity of adsorbents, the type of coverage and possibility of interaction between the adsorbate species. Adsorption data are usually described by adsorption isotherms, such as Langmuir, Freundlich and Temkin isotherms. These isotherms relate metal uptake per unit mass of adsorbent, q_e, to the equilibrium adsorbate concentration in the bulk fluid phase C_e [26].

Langmuir, Freundlich and Temkin isotherms and their linearized forms are shown in Figs. 9–11 respectively.

The linear regression was used to determine the best fit isotherm model.

The langmuir, Freundlich and Temkin adsorption constants estimated from the isotherms and the corresponding correlation coefficients are listed in Table 1. The highest regression correlation coefficient (0.9886) was observed for langmuir model, followed by Temkin (0.9578) and Freundlich (0.9334) models.

The R^2 values in the above table shows that the sorption of ammoniacal nitrogen on SB is monolayer sorption rather than the heterogeneous surface sorption energy distribution. This means that there is formation of monolayer coverage of ammonium molecules at the outer surface of the adsorbent.

3.4. Kinetic studies

The dynamics of sorption describes the rate of ammoniacal nitrogen adsorption on SB and this rate controls the equilibrium time. Information on the dynamics of sorption is required for selecting optimum operating condition for the full scale batch process [27]. In order to study the mechanism of sorption and potential rate determining steps, different kinetic models have been used to test experimental data obtained from 2 process variables. The sorption dynamics of the adsorption by SB as shown in Figs. 12 and 13 were tested with pseudo-first-order and pseudo-second-order kinetic models.

A linearized plot for the first order model is shown in Fig. 12. The Lagergren first-order rate constants k_1 and q_e were determined from the slope and y-intercept of the plot, respectively. These values are listed in Table 2. First-order kinetics failed to prove the proper fit dynamism for the adsorption of ammonium ion on SB.

Second-order plots resulted in straight line plot which led to determination of the second-order rate constants K_2 and q_e from the slope and y-intercept (Table 2). The R^2 value for the second-order kinetic model was 0.9652, while that for the first-order kinetic model was 0.5332. Thus, second-order kinetics provided the best fit for the kinetic data.

Table 1
Equilibrium isotherm parameters for adsorption of ammoniacal nitrogen onto SB

Langmuir isotherm	Freundlich isotherm	Temkin isotherm
$q = 833.333$	$n = 0.5821$	$A_T = 0.021792$
$K_m = -0.3871$	$K_f = 0.006224$	$b_T = 24356.35$
$R^2 = 0.9886$	$R^2 = 0.9334$	$R^2 = 0.9578$

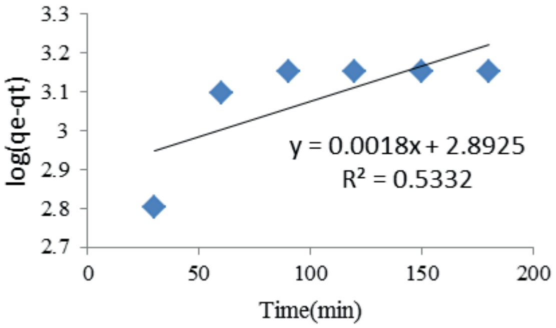

Fig. 12. Lagergren pseudo-first-order kinetic model for adsorption of ammoniacal nitrogen onto SB.

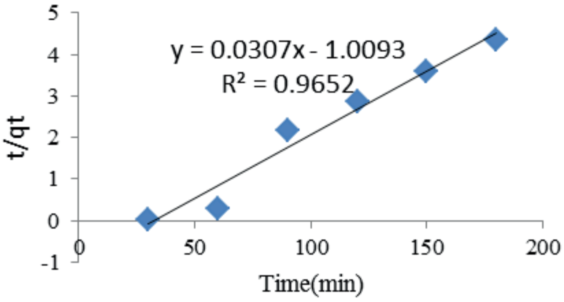

Fig. 13. Lagergren pseudo-second-order kinetic model for adsorption of ammoniacal nitrogen onto SB.

Table 2
Kinetics constants for adsorption of ammoniacal nitrogen onto SB

Pseudo-first order	Pseudo-second order
$K_1 = 0.004145$	$K_2 = 0.000934$
$q_e = 18.029$	$q_e = 32.57$
$R^2 = 0.5332$	$R^2 = 0.9652$

This second-order best fit result indicates that the 1:2 stochiometry binding with respect to monovalent binding site exists in the present system.

Comparable results were observed while working with brown alga *Sargassum*. They also compared both the orders of kinetics and found the second-order superior for the binding of the divalent cation to alga [28].

4. Conclusion

Removal of ammoniacal nitrogen from aqueous solutions using commercially available GAC and PAC are extensively worked. Utilization of agricultural waste is also quoted in the literature. Efforts in present study were to adsorption of ammonical nitrogen from wastewater using biomass that is, SB. With the optimum parameters, the adsorption reached a maximum of 97% removal of ammoniacal nitrogen. The main mechanism involved in the removal of ammonium ion is the complexation with the carboxyl and hydroxyl groups [29]. Isotherm studies revealed the data fit Langmuir's model indicating the formation of monolayer coverage of sorbate on the outer surface of the adsorbent. Also, the second-order kinetic model best fit with a correlation value nearer to 1 indicates that 1:2 stochiometry binding with respect to monovalent binding site exists in the present system [30,31]. The overall results suggest that the SB can be an attractive option for ammoniacal nitrogen removal from industrial wastewaters.

Acknowledgments

The authors wish to greatly acknowledge the financial support from Department of Science and Technology (DST) for the performance of present investigation studies as a part of the project under WOS-A scheme.

We are also grateful to L.M. College of Pharmacy, Ahmedabad and Sophisticated Instrumentation Centre for Applied Research and Testing – SICART, Anand for providing the FT-IR facility and Scanning Electron Microscope for the respective analysis.

References

[1] M. Suneetha, K. Ravindhranath, Removal of ammonia from polluted waters using biosorbents derived from powders of leaves, stems or barks of some plants, Pharm. Chem., 4 (2012) 214–227.
[2] K.O. Soetan, C.O. Olaiya, O.E. Oyewole, The importance of mineral elements for humans, domestic animals and plants: a review, Afr. J. Food Sci., 4 (2010) 200–222.
[3] S. Hussain, H. Abdul Aziz, M. Hasnain Isa, M.N. Adlan, F.A.H. Asaari, Physico-chemical method for ammonia removal from synthetic wastewater using limestone and GAC in batch and column studies, Bioresour. Technol., 98 (2006) 874–880.
[4] AWWA, Water Quality and Treatment, McGraw-Hill, New York, 1990.
[5] M. Rozic, S. Cerjan-Stefanovic, S. Kurajica, V. Vancina, E. Hodzic, Ammoniacal nitrogen removal from water by treatment withclays and zeolites, Water Res., 34 (2000) 3675–3681.
[6] Metcalf and Eddy Inc, Wastewater Engineering: Treatment, Disposal and Reuse, 4th ed. McGraw-Hill Co., New York, 2004.
[7] M.A. Wahab, S. Jellali, N. Jedidi, Effect of temperature and pH on the biosorption of ammonium onto *Posidonia oceanica* fibers: equilibrium, and kinetic modeling studies, Bioresour. Technol., 101 (2010) 8600–8615.
[8] APHA, AWWA, WPCF, Standard Methods for the Examination of Water and Wastewater, 18th ed. American Public Health Association, Washington, DC, USA, 1992.
[9] M.A. Wahab, S. Jellali, N. Jedidi, Ammonium biosorption onto sawdust: FTIR analysis, kinetics and adsorption isotherms modeling, Bioresour. Technol., 101 (2010) 5070–5075.
[10] Q. Du, S. Liu, Z. Cao. Y. Wang, Ammonia removal from aqueous solution using natural Chinese clinoptilolite, Sep. Purif. Technol., 44 (2005) 229–234.
[11] H. Zheng, L. Han, H. Ma, Y. Zheng, H. Zhang, D. Liu, S. Liang, Adsorption characteristics of ammonium ion by zeolite, J. Hazard. Mater., 158 (2008) 577–584.
[12] H. Nimenya, A. Delaunois, S. Bloden, D.L. Duong, B. Canart, P. Gustin, B. Nicks, M. Anasay, Ionic adsorption of ammonium and nitrate on some animal litters and their role in ammonia volatilization, Laboratory results, Ann. Zootech., 49 (2000) 129–140.
[13] M. Mishra, J.N. Tripathi, R.P. Singh, Utilization of agrowaste material as potential adsorbent for water treatment at different temperature, Indian J. Sci. Res., 4 (2013) 159–161.
[14] R. Nadeem, T.M. Ansari, A. Mukhtar, Fourier transform infrared spectroscopic characterization and optimization of Pb(II) biosorption by fish (*Labeo rohita*) scales, J. Hazard. Mater., 156 (2008) 64–73.

[15] H. Liu, Y. Dong, H. Wang, Y. Liu, Adsorption behavior of ammonium by a bioadsorbent- Boston ivy leaf powder, J. Environ. Sci., 22 (2010) 1513–1518.

[16] N.K. Mondal, R. Bhaumik, T. Baur, B. Das, P. Roy, J.K. Datta, Studies on deflouidation of water by tea ash: an unconventional biosorbent, Chem. Sci. Trans., 1 (2012) 239–256.

[17] Z. Zhang, I.M. O'Hara, G.A. Kent, W.O.S. Doherty, Comparative study on adsorption of two cationic dyes by milled sugarcane bagasse, Ind. Crops Products, 42 (2013) 41–49.

[18] S. Lagergren, About the theory of so-called adsorption of soluble substances, Kungliga Svenska Vetenskapsakademiens Handlingar, 24 (1898) 1–39.

[19] Y.S. Ho, G. McKay, Sorption of dye from aqueous solution by peat, Chem. Eng. J., 70 (1998) 115–124.

[20] Y.S. Ho, G. McKay, The kinetics of sorption of divalent metal ions ontosphagnum moss peat, Water Res., 34 (2000) 735–742.

[21] M.I. Temkin, V. Pyzhev, Kinetics of ammonia synthesis on promoted iron catalyst, Acta Phys. Chim., (1940) 327–356.

[22] C. Aharoni, M. Ungarish, Kinetics of activated chemisorption. Part 2. Theoretical models, J. Chem. Soc. Faraday Trans., 73 (1977) 456–464.

[23] M.A. Wahab, S. Jellali, N. Jedidi, Ammonium biosorption onto sawdust: FTIR analysis, kinetics and adsorption isotherms modelling, Bioresour. Technol., 101 (2010) 5070–5075.

[24] P. Senthil Kumar, K. Kirthika, Equilibrium and kinetic study of adsorption of nickel from aqueous solution onto bael tree leaf powder, J. Eng. Sci. Technol., 4 (2009) 351–363.

[25] A. Obiora-Okafo Ifeoma, O.D. Onukwuli, Utilization of sawdust (Gossweilerodendron balsamiferum) as an adsorbent for the removal of total dissolved particles from wastewater, Int. J. Multidisc. Sci. Eng., 4 (2013) 45–53.

[26] F. Deniz, S.D. Saygideger, Equilibrium, kinetic and thermodynamic studies of Acid Orange 52 dye biosorption by Paulownia *tomentosa* Steud. leaf powder as a low cost natural adsorbent, Bioresour. Technol., 101 (2010) 5137–5143.

[27] R. Hema Krishnaand, A.V.V.S. Swamy, Investigation on the effect of particle size and adsorption kinetics for the removal of Cr(vi) from the aqueous solutions using low cost sorbent, Eur. Chem. Bull., 1 (2012) 258–262.

[28] S. Swapna Priya, K.V. Radha, Batch adsorption studies of chromium(III) onto commercial grade granular activated carbon: equilibrium and kinetic studies, Int. J. Eng. Dev. Res., 13 (2013) 125–129.

[29] M. Kobya, Removal of Cr (VI)from aqueous solution by adsorption onto hazelnut shell activated carbon kinetic and equilibrium studies, Bioresour. Technol., 91 (2004) 317–321.

[30] V.K. Gupta, S.K. Strivastava, D. Mohan, Sorption dynamics, process optimization, equilibrium uptake and column operations for the removal and recovery of malachitc green using activated carbon and activated slag, Ind. Eng. Chem. Res., 36 (1994) 5539–554.

[31] C.C.V Cruz., A.C.A. da Costa, C.A. Henriques, A.S. Luna, Kinetic modeling and equilibrium studies during cadmium biosorption by dead *Sargassum* sp. Biomass, Bioresour. Technol., 91 (2004) 249–257.